RESEARCH ARTICLE | MARCH 18 2025

Electro-optic time transfer with femtosecond stability

Joshua Olson ; Robert Rockmore ; Nathan D. Lemke ; Sean Krzyzewski ; Brian Kasch

Appl. Phys. Lett. 126, 111103 (2025)
https://doi.org/10.1063/5.0240786

Applied Physics Letters ARTICLE pubs.aip.org/aip/apl

Electro-optic time transfer with femtosecond stability

Cite as: Appl. Phys. Lett. **126**, 111103 (2025); doi: 10.1063/5.0240786
Submitted: 11 October 2024 · Accepted: 10 February 2025 ·
Published Online: 18 March 2025

Joshua Olson,[1,a)] Robert Rockmore,[2] Nathan D. Lemke,[3] Sean Krzyzewski,[2] and Brian Kasch[2]

AFFILIATIONS

[1]Space Dynamics Laboratory, Utah State University, North Logan, Utah 84341, USA
[2]Space Vehicles Directorate, Air Force Research Laboratory, Albuquerque, New Mexico 87116, USA
[3]Department of Physics and Engineering, Bethel University, St. Paul, Minnesota 55112, USA

[a)]**Author to whom correspondence should be addressed:** joshua.l.olson@sdl.usu.edu

ABSTRACT

Optical two-way time and frequency transfer (O-TWTFT) is an enabling technology that has applications ranging from fundamental investigations of relativity to the operation of global navigation satellite systems. Linear-optical-sampling (LOS) between optical frequency combs has been used to create very stable optical two-way time and frequency transfer links over free-space. Here, we demonstrate two-way time and frequency transfer using LOS between electro-optic frequency combs. This two-way electro-optic time and frequency transfer system demonstrated instabilities as low as 15 fs at 1 s of averaging time. These results show a pathway to highly stable, frequency agile, and low SWaP-C time transfer networks.

Comparison between distant optical clocks could lead to new understanding about the nature of gravity,[1,2] improve global navigation satellite systems (GNSS),[3] enable precise geodetic mapping,[4] and reduce clock-based inaccuracies in very long baseline interferometry.[5,6] Deployed optical clock networks would consist of highly stable optical references, along with highly precise optical frequency dividers and free-space optical time-transfer transceivers.[1,2,7] The significant cost of deploying such timing networks has also motivated the miniaturization and power reduction of key optical components. With the demonstration of chip-scale components for optical references and stabilized optical clockwork,[8,9] similarly high performing methods for comparing these optical clocks will be required that have a path to full photonic integration.

Two-way time and frequency transfer methods use timing signals traveling over reciprocal paths. Departure and arrival times are measured independently at both local and remote sites and then compared to each other to remove the common time delay of the reciprocal path. This methodology has been well established using radio frequency (RF) carrier signals to transfer time between satellites.[10] The accuracy of this method was improved by over an order of magnitude by using pulsed lasers as a timing signal,[7,11] reaching sub-picosecond stability over 100 s in a laboratory demonstration.[11] Recent work has demonstrated sub-picosecond level stability using RF modulation of optical carrier signals.[12–14] The stability of these RF-over-optical time-transfer demonstrations are limited to a few hundreds of femtoseconds.

Low noise mode-locked fibers have been used to generate highly stable time-transfer links. Sub-femtosecond time synchronization over a fiber network has been achieved using low-noise mode-locked fiber oscillators locked to a microwave reference.[15] Optical two-way time and frequency transfer (O-TWTFT) with sub-femtosecond stability has been demonstrated in free space using linear-optical sampling (LOS)[16,17] between optical frequency combs (OFC) generated from fully stabilized mode-locked fiber lasers.[18–24]

OFCs can also be generated using direct electro-optic (EO) modulation of an optical carrier with RF signals.[25–30] Electro-optic (EO) combs are well suited to applications that benefit from accessing a large range of repetition rates, fast frequency switching, predictable output over a wide temperature range, or a flat optical spectrum.[31] As a result, EO comb generators have been implemented for gas sensing,[32,33] optical communications,[34] and as frequency references for astronomical spectroscopy.[35,36] EO comb generators have a path to significant SWaP-C improvements through on-chip photonic integration.[37–42] EO combs make a compelling option for optical time and frequency transfer because of their frequency tunability, agility, and the potential for photonic integration for scalable manufacturing.

In this work, we use LOS between two highly tunable EO comb generators to demonstrate O-TWTFT over a 1 km fiber optical link within a single laboratory. This demonstration uses a single clock that is common to both the local and remote nodes of the optical link to isolate the additive timing noise of the EO combs. This technique employs RF modulation of an optical carrier using fiber-coupled phase modulators, but we are able to achieve an improved noise floor over other RF over optical techniques by using LOS and low noise single tone RF synthesizers. After cancelation of the timing error induced by the optical link, stability below 15 fs is reached after 1 s of averaging. 15 fs stability is maintained with link attenuation as high as 40 dB. This proof-of-principle demonstration provides a compelling case for the use of two-way electro-optic time transfer (EOTT) for deployed time-transfer networks.

We compare time interval information between clocks in our system using LOS between remote and local EO combs. LOS temporally magnifies the terahertz electric field oscillations of the combs so the field information can be measured with a single photodetector and RF electronics. Furthermore, the picosecond level sensitivity limit set by photodetection timing jitter is surpassed by magnifying the optical timing noise above the back-end timing noise floor.[18,23] Temporal magnification is produced by generating two combs with offset repetition rates: a local comb with repetition rate, $f_{r,L} = f_r$, and a remote comb with repetition rate, $f_{r,R} = f_r + \Delta f_r$. The repetition rate offset produces a temporal walk-off between the pulse trains creating a cross correlation signal, a time-domain interferogram, that carries information about the relative timing and phase between the two frequency combs. The LOS magnification factor, M, is given by the ratio: $f_r/\Delta f_r$. As a result of the walk-off between pulse trains, many pulses do not contribute to the interferogram signal, decreasing the power efficiency when compared to other optical-time transfer methods.[43,44]

The interferogram signal is detected at a rate equal to Δf_r, which is the maximum update rate of the time transfer link. Figures 1(d)–1(f) show a record of the time-domain interferograms where f_r was set to 200 MHz and Δf_r is tuned to 1, 10, and 100 kHz. Measurements of the arrival time of the time-domain interferograms are made at both the local node, τ_L, and the remote node, τ_R. These measurements include information about time interval differences between the clocks at each node, τ_{LR}, time-of-flight noise in the common-path optical link, and residual measurement errors. Assuming reciprocity of the link, time-of-flight noise is common to measurements. As a result, τ_{LR} can be isolated from the time-of-flight noise by adding the time-interval measurements from the local and the remote node such that

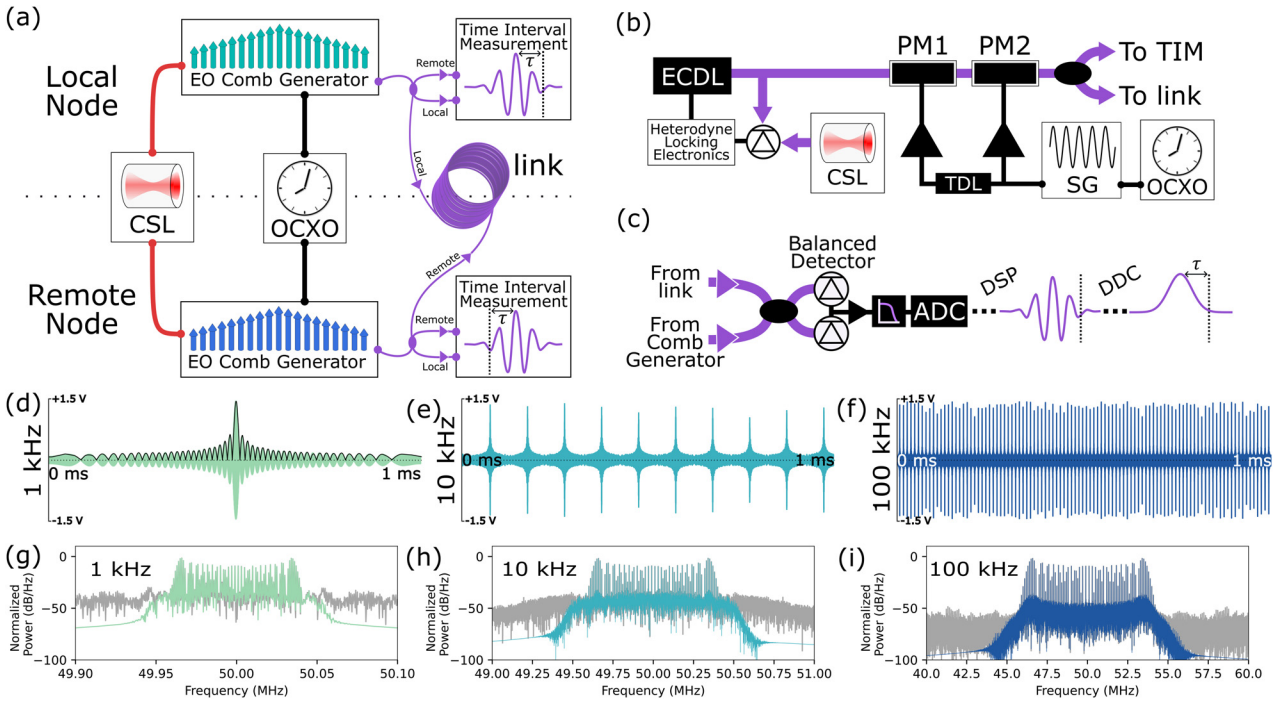

FIG. 1. (a) Overview of the EOTT system. Linear optical sampling between two EO combs is performed on two ends of a 1 km fiber optical link. The EO combs are individually generated at the remote node and the local node and share both an optical reference from a common CSL and an RF reference from an OCXO. (b) Diagram of an EO comb generator. An ECDL is locked to a CSL and is phase modulated to generate an EO comb. The phase modulators (PM) are driven by an amplified RF tone from an RF signal generator (SG). TDL: tunable RF delay line and TIM: time interval measurement. (c) Diagram of the time-interval measurement system. Light from one EO comb generator is coupled with light the EO comb generator that has traversed the optical link. The coupled light is detected on a balanced photodiode. After a LPF, the signal is digitized on an ADC. Digital signal processing (DSP) increases the SNR, and digital-downconversion (DDC) removes the carrier frequency before peak detection. (d)–(f) 1 ms time record of LOS interferograms produced with repetition rate differences of (d) 1 kHz, (e) 10 kHz, and (f) 100 kHz. Time records are shown after a digital BPF. (g)–(i) Interferogram spectra with repetition rate differences of (g) 1 kHz, (h) 10 kHz, and (f) 100 kHz. The interferogram spectra are shown both before (gray) and after applying a digital BPF.

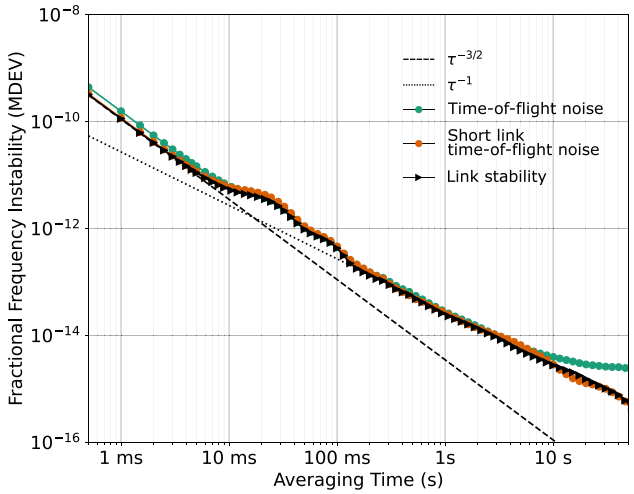

FIG. 2. Modified Allan deviation (MDEV) measurement of the fractional frequency instability of the system. (Green, squares) Time-of-flight noise of the 1 km fiber optic link shows the noise floor of a one-way time transfer system. (Orange, circles) Time-of-flight noise measurement over a shortened (1 m) fiber optic link shows that the increase in instability of the 1 km time-of-flight above 10 s of averaging time is due to technical noise fluctuations in the long link. (Black, triangles) 1 km link stability measurement using the two-way time-interval comparisons that removes common mode technical noise fluctuations of the long link. (Dashed) Expected MDEV slope for white phase noise. (Dotted) Expected MDEV slope for flicker phase noise.

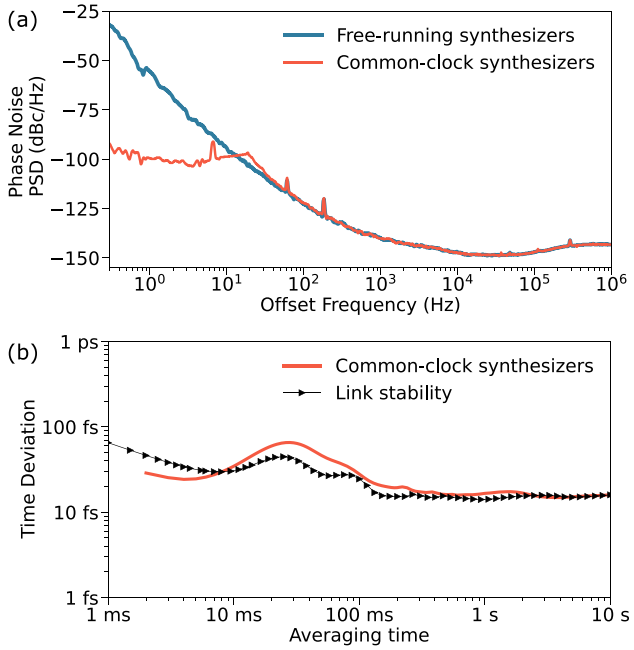

FIG. 3. (a) Relative phase noise measurement of the RF synthesizers generating a 200 MHz tone in a free-running configuration (blue) and a common-clock configuration (orange). (b) Calculated time deviation of the link (black) compared to the time deviation between the two RF synthesizers generating 200 MHz tones in a common-clock configuration (orange).

$$\frac{\tau_L + \tau_R}{2} = \tau_{LR} + \epsilon_\tau. \quad (1)$$

The combined residual timing error from measurements at the local and remote sites, ϵ_τ, limits the total link stability. Due to the shared clock between local and remote sites, $\tau_{LR} = 0$ and the comparison between time-interval measurements made at each site in Eq. (1) provides a direct calculation of the additive noise from the EOTT apparatus.

The experimental apparatus is shown in Fig. 1(a). The experiment includes two EO comb generators, one generator for the local node, and one for the remote node of our system. The optical reference in this experiment is derived from a single-frequency laser diode locked to an ultra-stable optical cavity. This cavity stabilized laser (CSL) is used as an optical reference to stabilize two external-cavity diode lasers (ECDLs), which are then used to generate the local and remote EO combs. The RF reference is derived from a commercially available oven-controlled crystal oscillator (OCXO). This OCXO is used to synchronize (1) the offset locks between the ECDLs and the CSL; (2) the RF signal that is used to generate sidebands around the EO comb carrier frequency; and (3) the onboard clock of the digitizer used to measure the timing information from the two combs. Other than the CSL, the OCXO, and the use of a single multichannel analog-to-digital converter, all the components in the two nodes of the system are completely independent. The EO combs are generated by phase modulating 1556 nm light from each ECDL in a series of two electro-optic (EO) phase modulators producing combs with 16 GHz of optical bandwidth. The phase modulators are driven by amplified signals from phase-lock loop (PLL) based RF synthesizers. Figure 3(a) shows the measured phase noise of the RF synthesizers when generating a 200 MHz tone.

The output of the local EO comb is split using fiber-optical couplers, and a part of the light is directed over a spooled 1 km fiber-optical cable [Fig. 1(a)]. At the other end of this fiber-optical link, at the remote node, the light is combined with the remote EO comb signal using a 50:50 fiber-optical coupler. This combined local and remote light is then sent to a balanced photodetector as shown in Fig. 1(c). The light from the remote EO comb is also split and sent across the fiber-optical link in the opposite direction before being combined with the local EO comb and similarly detected on a balanced photodetector at the local node. The EO comb generators produce highly chirped optical frequency combs, with frequency components

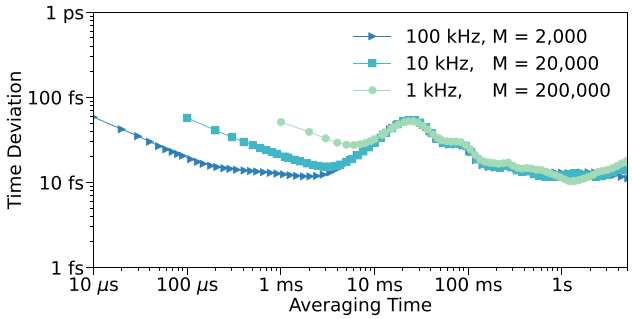

FIG. 4. Measurement of the time deviation over the 1 km fiber optical link with different link updates rates (repetition rate differences, Δf_r). Triangles: 100 kHz updates rate; squares: 10 kHz update rate; and circles: 1 kHz update rate.

spread out over the 5 ns period of the driving frequency. The ~2 ps differential time delay between optical frequency components across the comb bandwidth produced by the 1 km single-mode fiber was small compared to the initial differential time delay of each comb's optical frequency components, and therefore, no link dispersion compensation was required.

The RF signal measured on the photodiodes is low-pass filtered at 100 MHz and digitized on a 14-bit analog-to-digital converter (ADC) with a sample rate of 200 MS/s. The data from the digitizer are streamed continuously, without gaps, to data storage and post-processed. Figures 1(d)–1(f) show a record of the time-domain interferograms. The time record data are digitally bandpass filtered to remove out of band photodetector noise [Figs. 1(g)–1(i)]. The peaks of the interferograms are found with sub-sample precision by performing a cubic spline interpolation around the five highest points in each interferogram.

Figure 2 shows the measured two-way instability over the 1 km optical link. For this measurement, the local comb is generated with a 200 MHz modulation frequency and the remote comb is generated with a modulation frequency of 200.002 MHz. This produces a 2 kHz repetition rate difference (Δf_r) between the local and remote EO combs. Above 5 ms of averaging time, the modified Allan deviation (MDEV) of the link decreases proportionally to τ^{-1}, except for two peaks above 25 ms, which are caused by PLLs in the RF signal generators. The τ^{-1} trend to the MDEV indicates that the system performance is limited by flicker phase noise above 100 ms. Beyond 7 s of averaging time, the time-of-flight noise of the optical link dominates the one-way time-interval measurement. The two-way measurement reduces this time-of-flight noise down to the τ^{-1} noise floor, which also corresponds very closely to the one-way measurement over a shortened 1 m fiber-optical link. The corresponding two-way time deviation measurement for the 1 km link is shown in Fig. 3(b), demonstrating a noise floor of just under 15 fs after 1 s of averaging.

The relative noise between the synthesizers was measured using a phase meter with one synthesizer acting as the reference and the other synthesizer acting as the device-under-test. Both synthesizers were tuned to 200 MHz for this measurement. Figure 3(a) shows the relative phase noise between the synthesizers in both a free-running configuration, with independent clocks, and in a common-clock configuration. At offset frequencies below 10 Hz, the phase noise levels off, indicating that the synthesizer PLLs are tracking the common clock on timescales longer than 100 ms. The time deviation between the synthesizers was also calculated using the phase meter and is shown in Fig. 3(b). The time deviation between the synthesizers in the common-clock configuration closely matches the time deviation noise floor of the EOTT link beyond 100 ms of averaging time indicating that the long-term stability of the EOTT link is limited by phase noise in the PLLs of the synthesizers.

Improvements in link stability may be possible by using optical methods of generating low-phase noise RF signals.[45,46] The noise floor of the system can be reached at shorter averaging times by tuning the repetition rate difference between the two combs to produce higher update rates. With a 100 kHz update rate, the system could reach the noise floor of 15 fs after averaging for 2 ms, as shown in Fig. 4.

This experiment was performed over an optical fiber link for experimental convenience, but by varying link loss, we can simulate performance over a free-space link, which incurs loss from long-range propagation in turbulent atmosphere.[47] To measure the performance of the system with high link loss, we added calibrated optical attenuators to the fiber optical link when operating with an update rate of 1 kHz. A matched filter was also applied to the digitized signals to increase the SNR of the received interferograms under significant link attenuation. We were able to add more than 40 dB of attenuation to the link with transmitted signal powers as low as 100 nW before degrading the performance of the system, as shown in Fig. 5(a). With received optical powers below 100 nW, the stability of the link begins to degrade due to a reduction in the signal-to-noise ratio of the measured interferograms. Below 100 nW of received optical power, the time deviation at 1 ms begins to increase, eventually increasing at a rate inversely proportional to the square root of the transmitted optical power: $\sigma(1\,ms) \propto 1/\sqrt{P_{link}}$ [Fig. 5(a)].

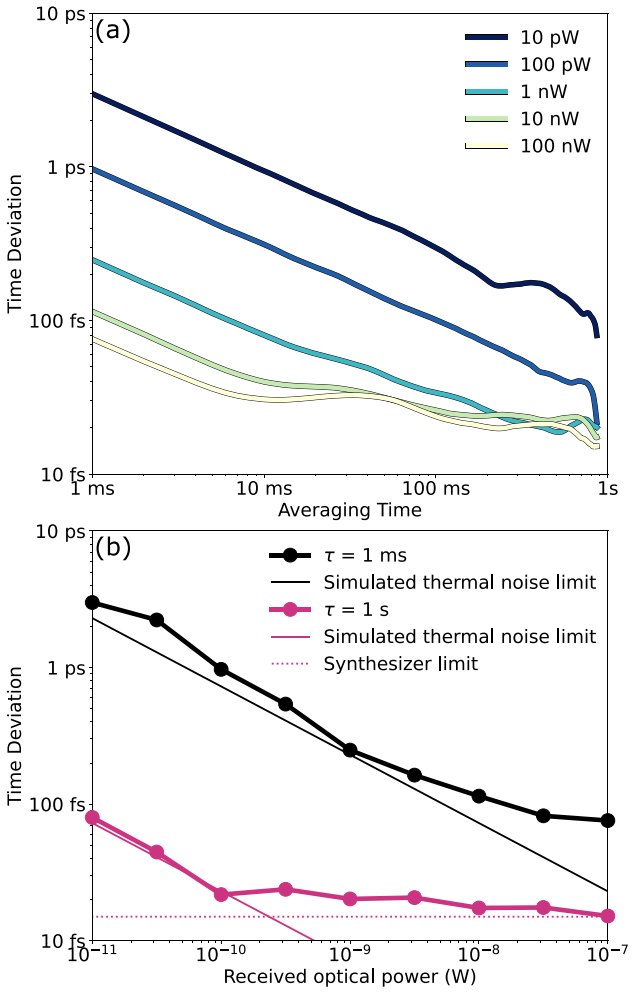

FIG. 5. (a) Measurement of link time deviation while the link is operating at an update rate of 1 kHz while attenuating the link signal. Link time deviations are shown at received optical powers from 10 pW to 100 nW in 10 dB increments. (b) Link time deviation measured at different received optical powers. Black dots: no averaging and pink dots: after 1 s of averaging. Photodetector noise limits are calculated from simulation; black, solid: no averaging, pink, solid: 1s of averaging, and pink, dotted: noise floor from the relative stability of the two RF synthesizers at 1 s of averaging.

To identify the noise source that caused this decreased stability, numerical simulation of the EO comb generators, optical link, and time-interval measurement was performed. In experiment, noise from the amplified balanced photodetectors was measured to have a nearly flat spectrum with a standard deviation of 1.9 mV after digitization. The digitizer sampled this noise at a rate of 200 MS/s, and 100 MHz low pass filters were used on the digitizer inputs. In simulation, white amplitude noise with this standard deviation was added to simulated interferograms measured at the same received optical powers that were observed in the experiment. Simulated interferogram arrival times were calculated using the same post-processing algorithm that was used to process the experimental data. A linear fit to the simulated deviation data was used to determine the detector noise limit and is shown in Fig. 5(b). The simulated noise limit from photodetector noise closely matches the noise limited performance of the system under large link attenuation, indicating that photodetector noise dominates at low received optical powers. Over long averaging times, some of this noise can be averaged down to reach better performance. Figure 5(b) shows that after 1 s of averaging, the stability of the system with 1 kHz update rate is mostly unaffected with received optical powers above 100 pW. Below 100 pW, the link stability at 1 s also begins to follow the photodetector noise limit.

The link was also tested with a 20 dB gain erbium-doped fiber amplifier (EDFA) added to the output of the EO comb generators, emitting 100 mW. The system performance with the EDFA included showed no performance degradation from amplified spontaneous emission, indicating that optical amplification could be used to establish long free-space optical links without decreasing the link stability.

In this work, we demonstrate a system for making two-way time interval measurements between clocks using LOS between electro-optic frequency combs. This EOTT method demonstrated a link stability of 15 fs with 1 s of averaging. This performance would represent at least an order of magnitude improvement in RF-over-optical time-transfer links when implemented in real time. Deployed time-transfer transceivers will be extremely sensitive to size, weight, power, and cost. For these applications, EOTT, with components that can be fully integrated on chip, has significant benefits. Furthermore, the wide frequency tuning range and frequency agility of EO comb generators can also provide a more flexible architecture for future time-transfer networks.

We thank Myles Silfies, Kyle Martin, Nader Zaki, and Steve Lipson for their careful reading of this manuscript.

The views expressed are those of the author and do not necessarily reflect the official policy or position of the Department of the Air Force, the Department of Defense, or the U.S. Government. Approved for public release; distribution is unlimited. Public Affairs release approval #AFRL20243924.

AUTHOR DECLARATIONS

Conflict of Interest

The authors have no conflicts to disclose.

Author Contributions

Joshua Olson: Conceptualization (supporting); Investigation (lead); Writing – original draft (lead); Writing – review & editing (lead). **Robert Rockmore:** Conceptualization (supporting); Funding acquisition (supporting); Writing – review & editing (supporting). **Nathan D. Lemke:** Investigation (supporting); Writing – review & editing (supporting). **Sean Krzyzewski:** Conceptualization (equal); Investigation (supporting); Funding acquisition (supporting); Writing – review & editing (supporting). **Brian Kasch:** Conceptualization (equal); Funding acquisition (lead); Writing – review & editing (supporting).

DATA AVAILABILITY

The data that support the findings of this study are available from the corresponding author upon reasonable request.

REFERENCES

[1]A. Derevianko, K. Gibble, L. Hollberg, N. R. Newbury, C. Oates, M. S. Safronova, L. C. Sinclair, and N. Yu, "Fundamental physics with a state-of-the-art optical clock in space," Quantum Sci. Technol. **7**, 044002 (2022).
[2]STE-Quest Team, "STE-Quest: Space-time explorer and quantum equivalance principle space test (assesment study report)," arXiv:2211.15412 (2013).
[3]P. Berceau, M. Taylor, J. Kahn, and L. Hollberg, "Space-time reference with an optical link," Classical Quantum Gravity **33**, 135007 (2016).
[4]J. Grotti, S. Koller, S. Vogt, S. Häfner, U. Sterr, C. Lisdat, H. Denker, C. Voigt, L. Timmen, A. Rolland, F. N. Baynes, H. S. Margolis, M. Zampaolo, P. Thoumany, M. Pizzocaro, B. Rauf, F. Bregolin, A. Tampellini, P. Barbieri, M. Zucco, G. A. Costanzo, C. Clivati, F. Levi, and D. Calonico, "Geodesy and metrology with a transportable optical clock," Nat. Phys. **14**, 437–441 (2018).
[5]C. Clivati, R. Aiello, G. Bianco, C. Bortolotti, P. D. Natale, V. D. Sarno, P. Maddaloni, G. Maccaferri, A. Mura, M. Negusini, F. Levi, F. Perini, R. Ricci, M. Roma, L. S. Amato, M. S. de Cumis, M. Stagni, A. Tuozzi, and D. Calonico, "Common-clock very long baseline interferometry using a coherent optical fiber link," Optica **7**, 1031–1037 (2020).
[6]M. Pizzocaro, M. Sekido, K. Takefuji, H. Ujihara, H. Hachisu, N. Nemitz, M. Tsutsumi, T. Kondo, E. Kawai, R. Ichikawa, K. Namba, Y. Okamoto, R. Takahashi, J. Komuro, C. Clivati, F. Bregolin, P. Barbieri, A. Mura, E. Cantoni, G. Cerretto, F. Levi, G. Maccaferri, M. Roma, C. Bortolotti, M. Negusini, R. Ricci, G. Zacchiroli, J. Roda, J. Leute, G. Petit, F. Perini, D. Calonico, and T. Ido, "Intercontinental comparison of optical atomic clocks through very long baseline interferometry," Nat. Phys. **17**, 223–227 (2021).
[7]E. Samain, D. Albanese, C. Courde, K. Djeroud, M. L. Bourez, S. Leon, H. Mariey, G. Martinot-Lagarde, J. L. Oneto, J. Paris, M. Pierron, P. Exertier, H. Viot, P. Guillemot, P. Laurent, F. Pierron, D. Rovera, J.-M. Torre, M. Abgrall, and J. Achkar, "Time transfer by laser link — T2L2: Current status and future experiments," in *2011 Joint Conference of the IEEE International Frequency Control and the European Frequency and Time Forum (FCS) Proceedings* (IEEE, San Francisco, CA, 2011), pp. 1–6.
[8]Z. L. Newman, V. Maurice, T. Drake, J. R. Stone, T. C. Briles, D. T. Spencer, C. Fredrick, Q. Li, D. Westly, B. R. Ilic, B. Shen, M.-G. Suh, K. Y. Yang, C. Johnson, D. M. S. Johnson, L. Hollberg, K. J. Vahala, K. Srinivasan, S. A. Diddams, J. Kitching, S. B. Papp, and M. T. Hummon, "Architecture for the photonic integration of an optical atomic clock," Optica **6**, 680 (2019).
[9]G. Moille, J. Stone, M. Chojnacky, C. Menyuk, and K. Srinivasan, "Kerr-induced synchronization of a cavity soliton to an optical reference for integrated frequency comb clockworks," arXiv:2305.02825 (2023).
[10]W. R. Stone, "TwoWay satellite time and frequency transfer (TWSTFT): principle, implementation, and current performance," in *Review of Radio Science 1996–1999* (IEEE, 2009).
[11]K. Schreiber, I. Prochazka, P. Lauber, U. Hugentobler, W. Schafer, L. Cacciapuoti, and R. Nasca, "Ground-based demonstration of the European Laser Timing (ELT) experiment," IEEE Trans. Ultrason., Ferroelectr., Freq. Control **57**, 728–737 (2010).
[12]I. Khader, H. Bergeron, L. C. Sinclair, W. C. Swann, N. R. Newbury, and J.-D. Deschênes, "Time synchronization over a free-space optical communication channel," Optica **5**, 1542 (2018).
[13]H. Yang, H. Wang, X. Wang, H. Yi, W. Yang, H. Wang, and S. Zhang, "Picosecond-precision optical two-way time transfer in free space using flexible binary offset carrier modulation," OSA Continuum **3**, 1264 (2020).

[14]F. Frank, F. Stefani, P. Tuckey, and P.-E. Pottie, "A sub-ps stability time transfer method based on optical modems," IEEE Trans. Ultrason., Ferroelectr., Freq. Control **65**, 1001–1006 (2018).
[15]M. Xin, K. Şafak, M. Y. Peng, A. Kalaydzhyan, W.-T. Wang, O. D. Mücke, and F. X. Kärtner, "Attosecond precision multi-kilometer laser-microwave network," Light Sci. Appl. **6**, e16187 (2016).
[16]C. Dorrer, D. Kilper, H. Stuart, G. Raybon, and M. Raymer, "Linear optical sampling," IEEE Photonics Technol. Lett. **15**, 1746–1748 (2003).
[17]I. Coddington, W. C. Swann, and N. R. Newbury, "Coherent linear optical sampling at 15 bits of resolution," Opt. Lett. **34**, 2153 (2009).
[18]F. R. Giorgetta, W. C. Swann, L. C. Sinclair, E. Baumann, I. Coddington, and N. R. Newbury, "Optical two-way time and frequency transfer over free space," Nat. Photonics **7**, 434–438 (2013).
[19]J.-D. Deschênes, L. C. Sinclair, F. R. Giorgetta, W. C. Swann, E. Baumann, H. Bergeron, M. Cermak, I. Coddington, and N. R. Newbury, "Synchronization of distant optical clocks at the femtosecond level," Phys. Rev. X **6**, 021016 (2016).
[20]H. Bergeron, L. C. Sinclair, W. C. Swann, C. W. Nelson, J.-D. Deschênes, E. Baumann, F. R. Giorgetta, I. Coddington, and N. R. Newbury, "Tight real-time synchronization of a microwave clock to an optical clock across a turbulent air path," Optica **3**, 441 (2016).
[21]L. C. Sinclair, H. Bergeron, W. C. Swann, I. Khader, K. C. Cossel, M. Cermak, N. R. Newbury, and J.-D. Deschênes, "Femtosecond optical two-way time-frequency transfer in the presence of motion," Phys. Rev. A **99**, 023844 (2019).
[22]Q. Shen, J.-Y. Guan, T. Zeng, Q.-M. Lu, L. Huang, Y. Cao, J.-P. Chen, T.-Q. Tao, J.-C. Wu, L. Hou, S.-K. Liao, J.-G. Ren, J. Yin, J.-J. Jia, H.-F. Jiang, C.-Z. Peng, Q. Zhang, and J.-W. Pan, "Experimental simulation of time and frequency transfer via an optical satellite–ground link at 10^{-18} instability," Optica **8**, 471 (2021).
[23]Q. Shen, J.-Y. Guan, J.-G. Ren, T. Zeng, L. Hou, M. Li, Y. Cao, J.-J. Han, M.-Z. Lian, Y.-W. Chen, X.-X. Peng, S.-M. Wang, D.-Y. Zhu, X.-P. Shi, Z.-G. Wang, Y. Li, W.-Y. Liu, G.-S. Pan, Y. Wang, Z.-H. Li, J.-C. Wu, Y.-Y. Zhang, F.-X. Chen, C.-Y. Lu, S.-K. Liao, J. Yin, J.-J. Jia, C.-Z. Peng, H.-F. Jiang, Q. Zhang, and J.-W. Pan, "Free-space dissemination of time and frequency with 10^{-19} instability over 113 km," Nature **610**, 661–666 (2022).
[24]K. W. Martin, M. S. Bigelow, N. Zaki, B. K. Stuhl, N. Matthews, J. D. Elgin, and K. Frey, "Demonstration of real-time precision optical time synchronization in a true three-node architecture," arXiv:2312.16348v1 (2023).
[25]T. Kobayashi, T. Sueta, Y. Cho, and Y. Matsuo, "High-repetition-rate optical pulse generator using a Fabry-Perot electro-optic modulator," Appl. Phys. Lett. **21**, 341–343 (1972).
[26]M. Kourogi, T. Enami, and M. Ohtsu, "A monolithic optical frequency comb generator," IEEE Photonics Technol. Lett. **6**, 214–217 (1994).
[27]M. Fujiwara, M. Teshima, J. Kani, H. Suzuki, N. Takachio, and K. Iwatsuki, "Optical carrier supply module using flattened optical multicarrier generation based on sinusoidal amplitude and phase hybrid modulation," J. Lightwave Technol. **21**, 2705–2714 (2003).
[28]C.-B. Huang, S.-G. Park, D. E. Leaird, and A. M. Weiner, "Nonlinearly broadened phase-modulated continuous-wave laser frequency combs characterized using DPSK decoding," Opt. Express **16**, 2520 (2008).
[29]A. J. Metcalf, V. Torres-Company, D. E. Leaird, and A. M. Weiner, "High-power broadly tunable electrooptic frequency comb generator," IEEE J. Sel. Top. Quantum Electron. **19**, 231–236 (2013).
[30]A. Metcalf, F. Quinlan, T. Fortier, S. Diddams, and A. Weiner, "Broadly tunable, low timing jitter, high repetition rate optoelectronic comb generator," Electron. Lett. **51**, 1596–1598 (2015).
[31]A. Parriaux, K. Hammani, and G. Millot, "Electro-optic frequency combs," Adv. Opt. Photonics **12**, 223 (2020).
[32]P. Martín-Mateos, B. Jerez, and P. Acedo, "Dual electro-optic optical frequency combs for multiheterodyne molecular dispersion spectroscopy," Opt. Express **23**, 21149 (2015).
[33]V. Durán, S. Tainta, and V. Torres-Company, "Ultrafast electrooptic dual-comb interferometry," Opt. Express **23**, 30557 (2015).
[34]H. Hu and L. K. Oxenløwe, "Chip-based optical frequency combs for high-capacity optical communications," Nanophotonics **10**, 1367–1385 (2021).
[35]X. Yi, K. Vahala, J. Li, S. Diddams, G. Ycas, P. Plavchan, S. Leifer, J. Sandhu, G. Vasisht, P. Chen, P. Gao, J. Gagne, E. Furlan, M. Bottom, E. C. Martin, M. P. Fitzgerald, G. Doppmann, and C. Beichman, "Demonstration of a near-IR line-referenced electro-optical laser frequency comb for precision radial velocity measurements in astronomy," Nat. Commun. **7**, 10436 (2016).
[36]K. Kashiwagi, T. Kurokawa, Y. Okuyama, T. Mori, Y. Tanaka, Y. Yamamoto, and M. Hirano, "Direct generation of 125-GHz-spaced optical frequency comb with ultrabroad coverage in near-infrared region by cascaded fiber configuration," Opt. Express **24**, 8120 (2016).
[37]C. Wang, M. Zhang, X. Chen, M. Bertrand, A. Shams-Ansari, S. Chandrasekhar, P. Winzer, and M. Lončar, "Integrated lithium niobate electro-optic modulators operating at CMOS-compatible voltages," Nature **562**, 101–104 (2018).
[38]M. He, M. Xu, Y. Ren, J. Jian, Z. Ruan, Y. Xu, S. Gao, S. Sun, X. Wen, L. Zhou, L. Liu, C. Guo, H. Chen, S. Yu, L. Liu, and X. Cai, "High-performance hybrid silicon and lithium niobate Mach–Zehnder modulators for 100 Gbit s-1 and beyond," Nat. Photonics **13**, 359–364 (2019).
[39]T. Ren, M. Zhang, C. Wang, L. Shao, C. Reimer, Y. Zhang, O. King, R. Esman, T. Cullen, and M. Lončar, "An integrated low-voltage broadband lithium niobate phase modulator," IEEE Photonics Technol. Lett. **31**, 889–892 (2019).
[40]Y. Hu, M. Yu, B. Buscaino, N. Sinclair, D. Zhu, R. Cheng, A. Shams-Ansari, L. Shao, M. Zhang, J. M. Kahn, and M. Lončar, "High-efficiency and broadband on-chip electro-optic frequency comb generators," Nat. Photonics **16**, 679–685 (2022).
[41]K. Han, D. A. Long, S. M. Bresler, J. Song, Y. Bao, B. J. Reschovsky, K. Srinivasan, J. J. Gorman, V. A. Aksyuk, and T. W. LeBrun, "Low-power, agile electro-optic frequency comb spectrometer for integrated sensors," Optica **11**, 392–398 (2024).
[42]K. Zhang, W. Sun, Y. Chen, H. Feng, Y. Zhang, Z. Chen, and C. Wang, "A power-efficient integrated lithium niobate electro-optic comb generator," Commun. Phys. **6**, 17 (2023).
[43]E. D. Caldwell, J.-D. Deschenes, J. Ellis, W. C. Swann, B. K. Stuhl, H. Bergeron, N. R. Newbury, and L. C. Sinclair, "Quantum-limited optical time transfer for future geosynchronous links," Nature **618**, 721–726 (2023).
[44]J. D. Roslund, A. S. Kowligy, J. Fujita, M. P. Ledbetter, A. V. Rakholia, M. M. Boyd, J. R. Abo-Shaeer, and A. Cingöz, "Optical two-tone time transfer," arXiv:2408.09290 (2024).
[45]X. Xie, R. Bouchand, D. Nicolodi, M. Giunta, W. Hänsel, M. Lezius, A. Joshi, S. Datta, C. Alexandre, M. Lours, P.-A. Tremblin, G. Santarelli, R. Holzwarth, and Y. Le Coq, "Photonic microwave signals with zeptosecond-level absolute timing noise," Nat. Photonics **11**, 44–47 (2017).
[46]M. Kalubovilage, M. Endo, and T. R. Schibli, "X-Band photonic microwaves with phase noise below -180 dBc/Hz using a free-running monolithic comb," Opt. Express **30**, 11266 (2022).
[47]A. Jahid, M. H. Alsharif, and T. J. Hall, "A contemporary survey on free space optical communication: Potentials, technical challenges, recent advances and research direction," J. Network Comput. Appl. **200**, 103311 (2022).